Materials & Design 222 (2022) 111097

Contents lists available at ScienceDirect

Materials & Design

journal homepage: www.elsevier.com/locate/matdes

Effects of modulation layer thickness on fracture toughness of a TiN/AlN-Ni multilayer film

Chao Zhou [a,1], Jingjing Wang [a,1], Jia Meng [b], Wei Li [a,*], Ping Liu [a], Ke Zhang [a], Fengcang Ma [a], Xun Ma [a], Rui Feng [c], Peter K. Liaw [d]

[a] School of Materials and Chemistry, University of Shanghai for Science and Technology, Shanghai 200093, PR China
[b] Key Laboratory of Inorganic Coating Materials, Chinese Academy of Sciences, Shanghai 200050, PR China
[c] Neutron Scattering Division, Oak Ridge National Laboratory, Oak Ridge, TN 37831, USA
[d] Department of Materials Science and Engineering, The University of Tennessee, Knoxville, TN 37996, USA

HIGHLIGHTS

- When the thickness of AlN-Ni layer is 2.4 nm, the TiN/AlN-Ni film behaves super-hardness and high toughness.
- The superhard effect is mainly caused by Koehler strengthening and alternating stress hardening.
- The formation of coherent interface and the AlN phase transformation are the key reasons for high toughness.

GRAPHICAL ABSTRACT

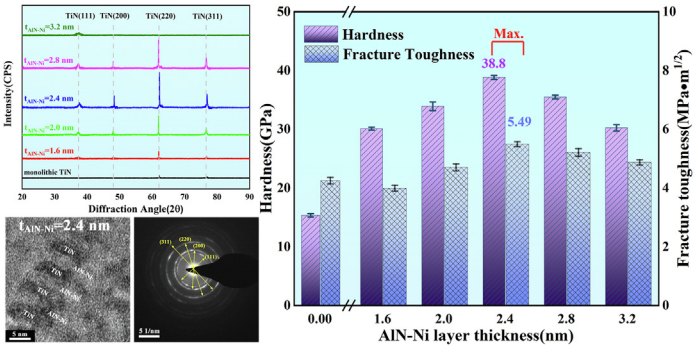

ARTICLE INFO

Article history:
Received 13 April 2022
Revised 23 August 2022
Accepted 23 August 2022
Available online 28 August 2022

Keywords:
TiN/AlN-Ni multilayer film
Modulation layer thickness
Hardness
Fracture toughness
Phase transformation

ABSTRACT

A series of TiN/AlN-Ni multilayer films with different modulation layer thicknesses were prepared by magnetron sputtering. Their microstructures and mechanical properties were characterized by X-ray diffraction (XRD), scanning electron microscopy (SEM), and high-resolution transmission electron microscopy (HRTEM). Therein, fracture toughness of multilayer films was determined by indentation method. The hardness and elastic modulus of all multilayers are greatly improved by introducing an AlN-Ni modulation layer. When the modulation-layer thickness is 2.4 nm, and the hardness and elastic modulus are the highest at the value of 39 GPa and 447 GPa, respectively, which is ascribed to Koehler strengthening and alternating stress hardening. Meanwhile the fracture toughness reaches the maximum, namely 5.49 MPa·m$^{1/2}$. It is attributed to the indentation-induced phase transformation of c-AlN to w-AlN and the formation of a good coherent interface. With further increasing the thickness of the AlN-Ni modulation layer, the multilayer film gradually becomes an amorphous structure, resulting in the decrease of hardness and toughness.

1. Introduction

Due to their excellent properties, such as high hardness, high melting point, good wear resistance, and corrosion resistance, multilayer films composed of transition metal nitrides (TMNs)

* Corresponding author.
E-mail address: liwei176@usst.edu.cn (W. Li).
[1] These authors contributed equally to this work.

https://doi.org/10.1016/j.matdes.2022.111097
0264-1275/

have been widely used in various tools and mechanical parts to prolong their service life [1–5]. Meanwhile, a multilayer film has been introduced into a metal gate and capacitor electrode materials in the micro-electro-mechanical system (MEMS) devices [6,7]. The size-dependent enhancement, that is, the change of the film hardness with a modulation period, Λ, has been widely studied [8–10]. However, the single high hardness of a multilayer film hardly suppressed cracking and failure when subjected to a large impact load, which largely limits its application in engineering. Therefore, the toughening of the hard multilayer film is an important engineering problem to be solved urgently in the current advanced manufacturing industry.

Generally, as the hardness of a hard film increases, the fracture toughness correspondingly decreases. Researchers have made a significant amount of efforts to overcome this difficulty. Various strengthening mechanisms, such as the grain refinement, Hall-Petch effects in various steels, and the nano-twin mechanism in high-entropy alloys, have opened up ways for the toughening of superhard coatings [11]. In recent years, researchers have focused on the development of new cermets with excellent hardness and toughness [12–14]. One of the popular schemes to improve film hardness and toughness is the design and construction of a multilayer structure. In this structure, structural phase transformation is considered to be effective in improving the toughness of the multilayer film. In the Cu/Ru multilayer film, there is a structural transformation between the face-centered-cubic (FCC) lattice and hexagonal-close-packed (HCP) lattices, which affects the length-scale-dependent cracking behavior and fracture toughness of the multilayer film [15]. The same toughening components of multilayer films or superalloy have been reported as TaC/Ag [16], a-CuZr/c-ZrN [17], Ni-625 [18], AlCrSiN/Ni [19], TiN/(Cr, Al)N [20], TiN/WN [21], and TaN/AlN [22].

In recent studies, it is mostly believed that superlattices have great potential in improving the toughness of TMNs films. A first-principles study has been conducted to simulate the super-toughness of several transition-metal nitride superlattice coatings (TiN/MN (M = V, Nb, Ta, Mo, and W)) [23]. The results showed that the in-plane Cauchy pressure of the TiN/MN superlattice was superior to other components. However, the modulation period of the model was only as thin as two atoms, and the arrangement of MN is close to the hexagonal structure at room temperature. Therefore, the ideal TiN/MN samples cannot be prepared in the experiment.

Apart from MN, aluminum nitride (AlN) is an alternative material for constructing various TMNs/AlN multilayer systems to obtain the expected high hardness and toughness. The commonly-used systems include TiN/AlN [24], CrN/AlN [25], and TaN/AlN [22], the performances of which depend on the phase structure of AlN. AlN exist in a cubic rocksalt structure (c-AlN) and hexagonal wurtzite structure (w-AlN) [26]. It has been confirmed that a phase transformation between w-AlN and c-AlN structure. Yalamanchili et al. [27] prepared a ZrN/$Zr_{0.63}Al_{0.37}N$ multilayer, where a rich ZrN and rich c-AlN phase separation occurs in the $Zr_{0.63}Al_{0.37}N$ layer, by reactive magnetron sputtering. The $Zr_{0.63}Al_{0.37}N$ layer with the c-AlN metastable phase kept a coherent epitaxial growth structure with ZrN when the thickness of the $Zr_{0.63}Al_{0.37}N$ layer was 2 nm. In the indentation test, the cubic structure, c-AlN, directly below the indentation was transformed into a hexagonal structure, w-AlN, under the effect of the stress induction, thus resulting in the enhanced fracture resistance. Based on these trends, the toughening effect was remarkable. Therefore, in the multilayer film with AlN as the modulation layer, the phase transformation of the AlN has an important effect on the toughening, which has great research prospects. However, the influence of the thickness of the AlN modulation layer on the phase transformation, which further affects toughness, has been less studied, and the internal mechanism is still vague.

Wang et al. [28]. Reported an Fe/VC multilayer coating, the bilayer period was set at 8 nm, and the Fe fraction varied from 0.6 to 0.9 Fe/VC multilayer coating with 90 % Fe fraction has almost twice the fracture toughness as the other Fe/VC coatings. They attributed the increase of toughness to the decrease of dislocation activation energy at the coherent interface of Fe/VC, which was conducive to dislocation movement. The same result was also confirmed in the study of Ranade et al. [29]. Zhang [30] reported nanocomposite films produced by a co-sputtering of Ti, TiNi and Si_3N_4 targets. When the doping amount of Ni increases from 0 to 40 %, the toughness of the films increases from 1.15 MPa·$m^{1/2}$ to 2.60 MPa·$m^{1/2}$. So, Ni can be doped into the film as a good ductile phase. And it is believed that nano-multilayers composed of materials with phase transformation characteristics are very worthy of study on the toughening of superhard films. Therefore, it is hopeful to study the effect of phase transition and coherent interface, which are adjusted by the thickness of modulation layer, on the toughening of multilayer films composed of TMNs and composite modulation layers.

In this study, TiN with an FCC structure was selected as the main layer, and AlN and Ni with the high hardness and excellent oxygen diffusion barrier effect were selected to form the composite-modulation layer, where Ni plays the role of a ductile phase. A series of TiN/AlN-Ni multilayer films with different thicknesses of modulation layers were prepared by magnetron sputtering technique. Through studying the microstructures and mechanical properties of the as-deposited multilayer films, the influence of the modulation layer thickness of on its fracture toughness is detected. Furthermore, the role of the AlN phase transformation in the toughening mechanism of multilayer films is discussed.

2. Experimental

2.1. Film preparation

The TiN/AlN-Ni multilayers were prepared on a monocrystalline silicon substrate by a multi-target magnetron sputtering system. High-purity titanium (Ti, 99.99 % weight percent) and aluminum nickel ($Al_{60}Ni_{40}$) composite targets were adopted, the Al:Ni volume ratio of which is 3:2. Firstly, the monocrystalline silicon wafers were ultrasonically cleaned with the anhydrous ethanol and acetone for 15 min, respectively. Before deposition, the base vacuum was pumped down to 4×10^{-3} Pa, and then argon and nitrogen gases were introduced into the chamber at the same flow rates of 15 standard-cubic-centimeter-*per*-minute (sccm). During deposition, the working pressure was maintained at 0.5 Pa. The Ti target was sputtered by the direct-current (DC) power with 150 W, whereas the Al-Ni target was sputtered by a radio-frequency (RF) power with 80 W. By controlling the deposition time of the main and modulation layers, the thickness of the TiN layer maintained at 5.0 nm, and the thickness of the AlN-Ni layer ranges from 1.6 nm to 3.2 nm. In addition, monolithic TiN films were also prepared with the same deposition parameters as a comparison.

2.2. Film characterization

The microstructure analysis of the TiN/AlN-Ni multilayer films was carried out with an X-ray diffractometer (XRD, D8 Advance XRD, CuKα radiation, λ = 0.15406 nm), the field emission scanning electron microscopy (SEM, FEI Quanta FEG 450) and field emission high-resolution transmission electron microscopy (HRTEM, FEI Tecnai G^2 20). The scanning range in the XRD measurement is from 20° to 90°. The hardness and elastic modulus of the films were measured by the Nano Indenter G200 nanometer instrument and

the Berkovich diamond indenter according to the Oliver-Pharr model [31]. The internal stress of the film was analyzed by the FST1000 film stress tester. The fracture toughness was calculated by the indentation method, and the formula is as follows [32]:

$$K_{IC} = \alpha\left(\frac{E}{H}\right)^{\frac{1}{2}}\left(\frac{P}{C^{\frac{3}{2}}}\right) \quad (1)$$

where α is a constant depending on the indenter geometry. Here, for the Berkovich indenter, α is 0.032. E and H are the elastic modulus and hardness of the films tested, respectively. P is the indentation load. Here, the indentation load is 5 mN. C is the crack length.

3. Results

3.1. Microstructure of the multilayer films

Fig. 1 exhibits the cross-sectional SEM images of the monolayer TiN film and some multilayer films. The monolayer TiN film shows obvious columnar growth. When the modulation layer thicknesses, $t_{AlN\text{-}Ni}$, are 1.6 nm and 2.4 nm, the columnar structure can still be clearly observed in the multilayer films. When $t_{AlN\text{-}Ni}$ is above 2.4 nm, the columnar structure gradually disappears and transforms into a dense structure, which is closely related to the microstructure evolution of the multilayer films.

The XRD patterns of the TiN/AlN-Ni multilayer films with different modulation layer thicknesses are shown in Fig. 2. When modulation layer thickness is 0, namely a monolithic TiN, there is weak (220) diffraction peak in XRD. The crystallinity of the TiN film is weak, almost showing an amorphous state. The large atomic-size difference is the main reason for the formation of an amorphous state [33]. After introducing an AlN-Ni composite modulation layer, the crystallinity of the films increases, which is concluded from the (111), (200), (220) and (311) diffraction peaks appearing in the XRD for the TiN/AlN-Ni multilayer films. Therein, when the thickness of the AlN-Ni layer is less than 2.4 nm, the AlN layer grows into metastable c-AlN under the template of the TiN layer, forming a good coherent interface with the TiN layer and grow epitaxially, which improves the crystallization integrality of nano-multilayers [10]. With the initial increase of the AlN-Ni layer thickness, the intensities of (111), (220) and (311) peaks gradually increase and reach the maximum value when the AlN-Ni layer thickness is 2.4 nm. However, when the thickness of AlN-Ni layer exceeds 2.4 nm, the intensities of (111), (220) and (311) peaks decrease, and the peaks shapes broaden, which means that the effect of improving the crystallization integrity gradually disappears, it is particularly obvious when $t_{AlN\text{-}Ni}$ = 3.2 nm. Thus, it is inferred that when the thickness of the AlN-Ni layer is 2.4 nm, the structure of the AlN phase will transform into an FCC structure under the action of the TiN template, and form a good coherent epitaxial growth with the TiN layer [34]. As the thickness of the AlN-Ni layer is 3.2 nm, the TiN layer begins to return to an amorphous structure, which destroys coherent growth. Moreover, it is worth noting that there is no diffraction peak in AlN-Ni layer, which can be attributed to the fact that AlN-Ni layer thickness is too small to produce enough diffraction density detected by XRD. Besides, when the thickness of the AlN-Ni layer reaches a specific value such as 2.4 nm, the structure of the AlN phase will transform into an FCC structure under the action of the TiN template, and form a good coherent epitaxial growth with the TiN layer. In this case, it will show a same structure with that of the template layer TiN. Based on the above two reasons, the XRD peaks from the AlN-Ni layers hardly appear.

In order to further detect the microstructures of the multilayer films, HRTEM is conducted by taking the example of TiN/AlN-Ni multilayer films with $t_{AlN\text{-}Ni}$ as 2.4 nm. Fig. 3 shows the cross-sectional HRTEM images and selected area electron diffraction (SAED) of the TiN/AlN-Ni multilayer film. The low-magnification image in the Fig. 3(a, b) clearly shows that the multilayer film has a good layered structure characterized by the main layer, TiN, and the modulation layer, AlN-Ni, which correspond to the dark and the bright regions, respectively. The thicknesses of TiN and AlN-Ni layers are 5.0 nm and 2.4 nm, respectively, which are in good agreement with the calculated values of the deposition rate and deposition time. Besides, it indicates the columnar structure grown in the film, which is consistent with the results from SEM. In the high-magnification image of Fig. 3(c), it can be seen that most of the lattice fringes continuously pass through the modulation layer and the interface, indicating that AlN is transformed into a cubic structure under the effect of a TiN template. Besides, it

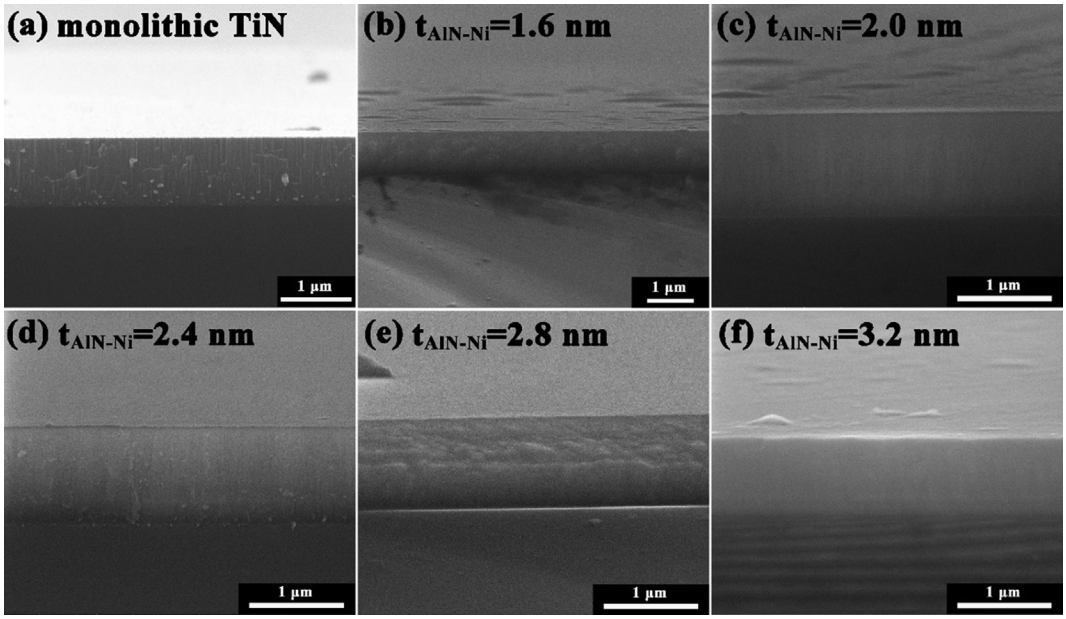

Fig. 1. Cross-sectional SEM images of the as-deposited films.

exhibits the formation of a coherent interface between the main layer and the modulation layer. The SAED pattern in Fig. 3(d) shows that the TiN phase in the TiN/AlN-Ni multilayer film completely presents the FCC structure. Meanwhile, it shows no diffraction characteristics of the AlN hexagonal structure, which is consistent with the results from XRD.

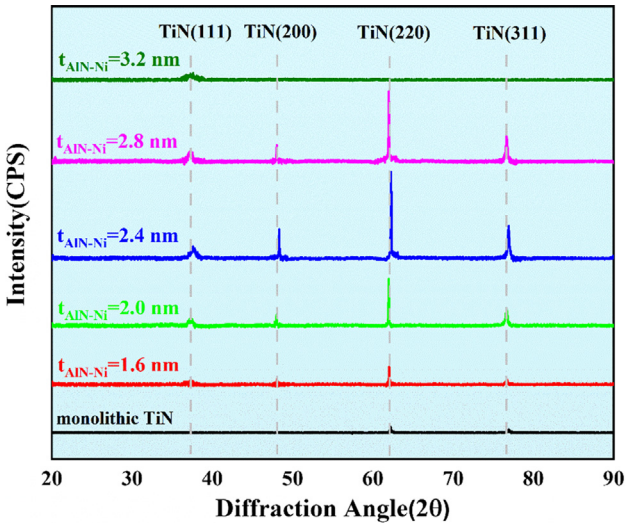

Fig. 2. XRD patterns of TiN/AlN-Ni multilayer films with different AlN-Ni layer thicknesses.

3.2. Mechanical properties of multilayer films

Fig. 4 shows the hardness and elastic modulus of the as-deposited films varying with the thickness of the AlN-Ni layer. The hardness and elastic modulus of the monolithic TiN film are 15.3 GPa and 227.5 GPa, respectively. However, the hardness and elastic modulus of the TiN/AlN-Ni multilayer films generally increase with introducing the AlN-Ni modulation layer, showing a trend of first increasing and then decreasing. When t_{AlN-Ni} = 2.4 nm, the hardness and elastic modulus of the multilayer film reach the maximum, which are 39.0 GPa and 467.3 GPa, respectively. When the thickness of the AlN-Ni layer exceeds 2.4 nm, the hardness and elastic modulus of the multilayer film decrease. The greater the difference between the shear moduli of the two layers, the more obvious the blocking of dislocation motion by the additional stress, and the more significant the strengthening effect of the nano-multilayer. The shear modulus (G) can be expressed as $G = E/2(1 + \nu)$ (E is the elastic modulus and ν is the Poisson's ratio). Using the above data for the monolithic film (E_{TiN} = 227.5 GPa, E_{AlN-Ni} = 84.3 GPa) and the Poisson ratio of 0.25, the shear moduli of TiN and AlN-Ni be respectively calculated as G_{TiN} = 91 GPa and G_{AlN-Ni} = 33.7 GPa. Therefore, the strengthening effect produced by the difference in shear modulus must be part of the reason for the increase in hardness and elastic modulus of the nano-multilayer films.

Fig. 5 displays the internal stress of the monolithic TiN and TiN/AlN-Ni multilayer films with different t_{AlN-Ni}. Here, the internal stress is calculated through the Stoney equation [35]. The results

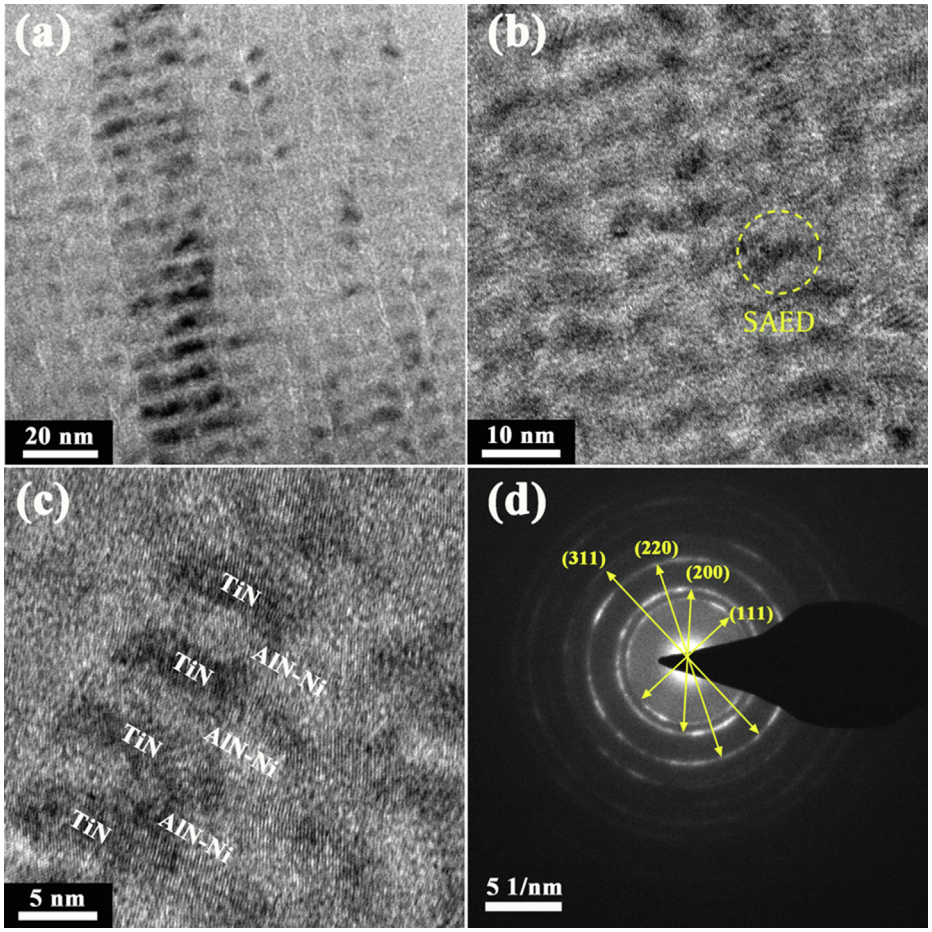

Fig. 3. Cross-sectional HRTEM images of TiN/AlN-Ni multilayer films: (a) low-magnification, (b) middle-magnification, (c) high-magnification, and (d) selected area diffraction pattern.

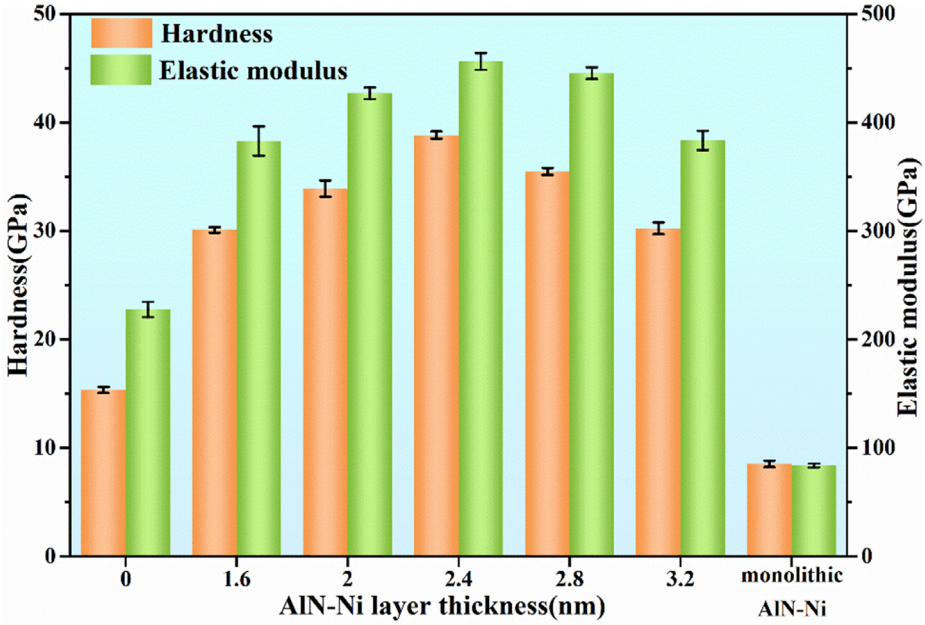

Fig. 4. Variation of hardness and elastic modulus of the as-deposited films with different AlN-Ni layer thicknesses.

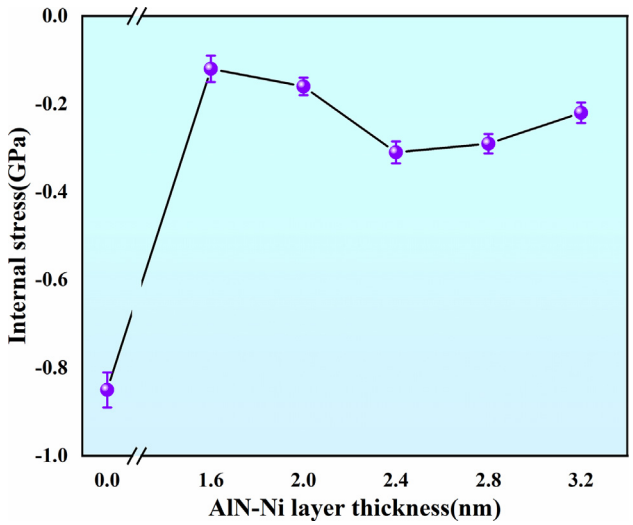

Fig. 5. The internal stresses of the as-deposited films with different AlN-Ni layer thicknesses.

show that all films sustained compressive stresses. The compressive stress of TiN monolayers reaches 0.85 GPa. However, the high stress of TiN monolayers can be effectively released by introducing the AlN-Ni modulation layer. With the increase of the AlN-Ni layer thickness, the compressive stress of the multilayer film first increases and then decreases. Yet it is still much lower than that of TiN monolayers. When the AlN-Ni layer thickness is 2.4 nm, the compressive stress is about 0.3 GPa.

3.3. Toughness of the multilayer films

Generally, the plastic-deformation resistance, H^3/E^2, is summarized as a toughness index [36], showing a similar trend to H and E. Therefore, it is seen from Fig. 4 that the superhard TiN/AlN-Ni multilayer film with t_{AlN-Ni} = 2.4 nm displays high toughness at the same time. Nevertheless, it is not enough to characterize the toughness only according to the relationship of H^3/E^2. In this study, the Berkovich indenter in the nanoindentation test was used for the indentation test to further evaluate the fracture toughness (K_{IC}) of the multilayer films. The corresponding SEM images of the indentation for some films are shown in Fig. 6. For the monolithic TiN film, many obvious radial cracks and extrusion cracks

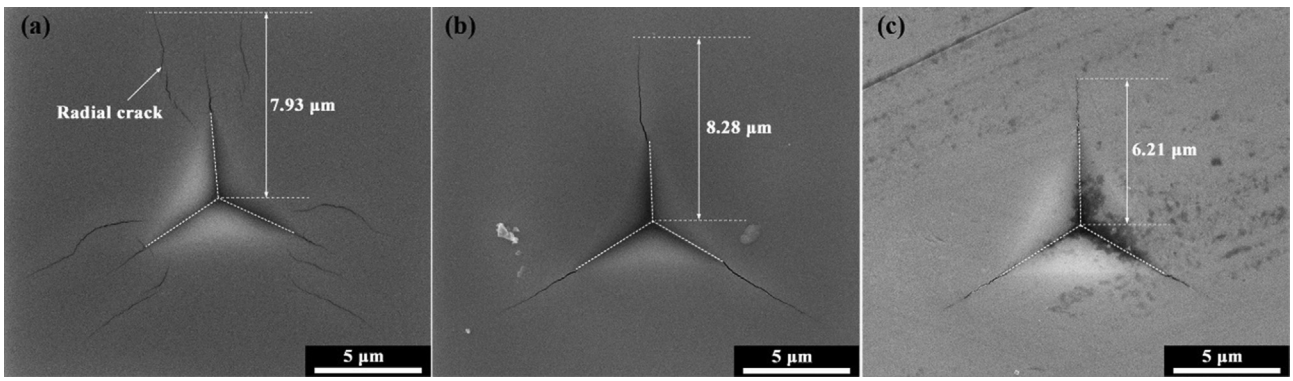

Fig. 6. SEM micrographs of indentation by the Berkovich indenter under a 1,000 nm depth for three films: (a) monolithic TiN film; (b) t_{AlN-Ni} = 1.6 nm, (c) t_{AlN-Ni} = 2.4 nm.

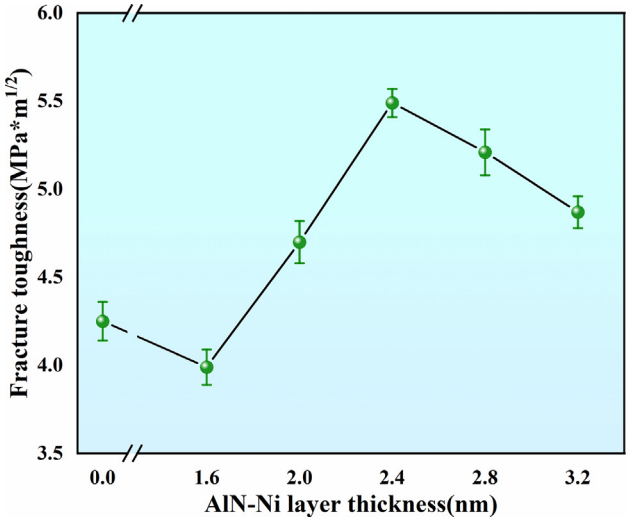

Fig. 7. The fracture toughness of TiN/AlN-Ni multilayer films with different AlN-Ni layer thicknesses.

can be seen, but only three radial cracks appearing in multilayer films. Particularly, when t_{AlN-Ni} is 2.4 nm, the length of the radial cracks becomes shortest (Fig. 6c), which is reduced from 8.28 μm to 6.21 μm. It is indicated that the multilayer film exhibits better fracture toughness under this modulation-layer thickness.

According to Eq. (1), the calculated values of K_{IC} are presented in Fig. 7. It is worth noting that when the thickness of the AlN-Ni layer is 1.6 nm, the fracture toughness of the nano-multilayer film is slightly lower than that of the monolithic TiN film. With the increase of the AlN-Ni layer thickness, the amorphous characteristics become weaker, and the crack propagation is inhibited [1]. When the thickness of the AlN-Ni layer is 2.4 nm, the multilayer film shows the highest fracture toughness, and the value of which is 5.49 MPa·$m^{1/2}$. When t_{AlN-Ni} is larger than 2.4 nm, the toughness decreases. Yet it is still higher than that of the monolithic TiN film.

4. Discussion

4.1. Influence of the AlN-Ni layer thickness on microstructures of films

It is well known that the stably-sputtered state of AlN is w-AlN. When preparing multilayer films with an AlN modulation layer, the AlN in the modulation layer can be transformed into c-AlN by controlling the modulation period [37,38]. The phase structure of AlN determines the interface structure (coherent, incoherent, or semi-coherent) of TiN/AlN-Ni multilayer films, which is closely related to the hardness and oxidation resistance of TiN/AlN-Ni nano-multilayer films.

The crystalline AlN-Ni layer can further promote the growth and crystal integrity of TiN layer, showing the increase of the XRD peak intensity. The same phenomenon was reported in other systems, such as the TiN/AlN [39], TaN/AlN [22], and NbN/AlN [40]. The stable structure of AlN is a hexagonal zincblende structure, and its transformation to a NaCl-cubic structure can only be achieved at room temperature and high pressure above 23 GPa [41]. When the thickness of AlN-Ni is less than 3 nm, AlN can be transformed into a cubic structure under the "template action" of TiN, maintaining co-epitaxial growth with the TiN layer. In the case of a thicker AlN-Ni layer, the peak intensity decreases rapidly with the increase of t_{AlN-Ni}. The most probable reason is that AlN gradually transforms into an amorphous structure under a thicker AlN-Ni layer and loses epitaxial growth with the TiN layer. When t_{AlN-Ni} is 2.4 nm, a good coherent interface is formed between AlN-Ni and TiN layers, which proves that the template effect occurs. The combined XRD and HRTEM results demonstrate that the AlN-Ni layer is fully crystallized and coherently grown with the TiN layer. The t_{AlN-Ni}-dependent crystallization of the TiN layer could be explained from the viewpoint of thermodynamics, where the total energy (E_{total}) of multilayer films per formula unit can be expressed as follows [40].

$$E_{total} = (E_B + E_s)t_{AlN-Ni} + E_i \quad (2)$$

where E_B, E_S, and E_i are the strain-free bulk energy, the coherency strain energy, and the interfacial energy, respectively. As the AlN-Ni layer is extremely thin ($\leq$ 2.4 nm), the E_i was the main contributor to the E_{total}. When the coherent interface is formed, the values of E_i, namely E_{total} will be lowered. Therefore, the AlN-Ni in the modulation layer prefer to grow epitaxially with the TiN layer in the FCC structure. When t_{AlN-Ni} increases beyond a critical value, E_B and E_S gradually occupy the dominant position of E_{total}. Because the E_B value of the c-AlN is larger than that of the w-AlN, the AlN in the modulation layer will be transformed back into w-AlN, thus destroying the coherent epitaxial growth.

4.2. The improvement of mechanical properties

The hardness and elastic modulus of the TiN/AlN-Ni multilayer films are much higher than those of the monolithic TiN film. When t_{AlN-Ni} is 2.4 nm, the multilayer film shows a maximum increase in hardness. The enhancement of hardness and elastic modulus can be explained by the theories, mainly including the Koehler's modulus-difference strengthening theory [42] and alternating stress-strengthening theory [43,44]. According to the Koehler's modulus-difference strengthening theory, when the dislocation passes through the interface of the multilayer films, the dislocation is hindered by the forces originated from different shear moduli of the two layers at the interface of multilayer films. The greater the difference between the shear modulus of the two layers, the more obvious the additional stress hinders the movement of dislocations, and thus, the more significant the strengthening effect of the multilayer films. Besides, according to alternating stress-strengthening theory, despite that the TiN and AlN-Ni both present the same structure in this study, they have the different lattice parameters. The lattice parameter of TiN is a = 4.241 Å, while those of AlN are a = 3.110 Å, c = 4.979 Å. Under the epitaxial growth structure, the AlN with the smaller lattice parameter is subjected to the tensile stress, while the TiN with the larger lattice parameter bears the compressive stress. As a result, the alternating compressive and tensile stress fields form, which can also restrain the dislocation motion and strengthen the TiN/AlN-Ni multilayer nano-multilayer film. Therefore, the synergetic strengthening mechanisms of modulus-difference strengthening theory and alternating stress-strengthening theory derived from different layers accounts for the high hardness for the TiN/ AlN-Ni multilayer with the AlN-Ni layer thickness of 2.4 nm. As the thickness of the modulation layer increases, the AlN-Ni phase hardly continuously crystallizes into a quasi-crystalline cubic structure, but grows into the original zincblende structure, resulting in a decrease in the hardness and elastic modulus. The similar phenomena also appear in many other nitride coatings, such as CrN/AlN [45], CrN/TiN [46], and VC/AlN [47].

The difference in the fracture behavior between the multilayer films can be attributed to the evolution of the interface structure, which has also been reported in other studies [48]. For the TiN monolayer film, due to the poor crystallinity, the crack propagation easily occurs during the indentation test. With the increase of t_{AlN-Ni}, the fracture toughness of the multilayer films first increases and then decreases. When t_{AlN-Ni} is 2.4 nm, the fracture toughness

reaches the maximum. The toughening mechanisms in the 2.4 nm AlN-Ni layer may include a favorable coherent interface and the indentation-induced transformation. Firstly, the alternating stress-field based on the coherent interface between the TiN layer and AlN-Ni layer will reduce the activation energy of the nearby dislocation movement, consequently improve toughness [28]. In Verma et al. [49], multilayer interfaces can provide additional stress relief mechanisms through layer slip, thereby reducing shear cracks, this result is consistent with references. According to Hahn et al. [12], a power-law relationship similar as for τ will hold between the fracture toughness and the bilayer period:

$$K_{IC} \propto \Lambda^{-m} \tag{3}$$

with the exponent m depending on the type and interface constitution of the superlattice structure. The exponent m equals roughly 0.25 for their superlattice TiN/CrN coatings with $\Lambda \geq 6.2$ nm. In this paper, when $t_{AlN\text{-}Ni}$ is 2.4 nm, the multilayer is coherent interfaces, and the Λ is 7.4 nm, which can also be explained by the above relationship.

Secondly, it is previously pointed out that the metastable c-AlN is well formed at the coherent interface for the multilayer film with $t_{AlN\text{-}Ni}$ = 2.4 nm. During indentation, stress fields induced by indentation will trigger the transformation of the metastable c-AlN to w-AlN along with a volume expansion of about 20 %, which leads to localized compressive stresses and inhibits crack initiation and crack propagation, producing a better fracture toughness. Previously, it has been suggested that the indentation-induced stress would cause the crystal rotation and dislocation glide, thereby providing the possibility for lattice reconstruction [27]. Therefore, the formation of the coherent interface and the phase transformation of c-AlN to w-AlN in the TiN/AlN-Ni multilayer films are the key factors for achieving the synergetic super hardness and high toughness.

5. Conclusions

The TiN/AlN-Ni multilayer films with different modulation layer thicknesses were prepared by reactive magnetron sputtering. The microstructure and mechanical properties (hardness and fracture toughness) of multilayer films were studied. The conclusions are summarized as follows:

(1) Compared to the monolithic TiN film, the introduction of the AlN-Ni modulation layer greatly improves the hardness and elastic modulus of all multilayer films. When the thickness of the AlN-Ni modulation layer is 2.4 nm, the hardness and toughness reach the maximum, and the values of which are 39.0 GPa and 467.3 GPa, respectively. All multilayer films are subjected to the compressive stress, which is greatly released, compared to the monolithic TiN film.

(2) When $t_{AlN\text{-}Ni}$ is 2.4 nm, the AlN layer grows into the metastable c-AlN under the template action of the TiN layer, forming a good coherent interface with the TiN layer. In the indentation experiment, it shows best resistance to crack growth, and the maximum toughness is 5.49 $MPa{\cdot}m^{1/2}$.

(3) The superhard effect observed in the TiN/AlN-Ni multilayer film is mainly caused by Koehler modulus-difference strengthening and alternating-stress hardening. The formation of coherent interface and the AlN-phase transformation in the TiN/AlN-Ni multilayer films are the reasons for the improvement of its toughness. The present work provides a new idea for the development of TiN-based multilayer films with high hardness and high toughness.

CRediT authorship contribution statement

Chao Zhou: Investigation, Data curation, Methodology, Visualization, Writing – original draft, Validation. **Jingjing Wang:** Visualization, Writing – original draft, Writing – review & editing. **Jia Meng:** Resources, Supervision. **Wei Li:** Conceptualization, Resources, Supervision, Project administration, Funding acquisition. **Ping Liu:** Supervision, Project administration. **Ke Zhang:** Resources, Supervision. **Fengcang Ma:** Resources, Supervision. **Xun Ma:** Resources. **Rui Feng:** Writing – review & editing. **Peter K. Liaw:** Writing – review & editing.

Data availability

Data will be made available on request.

Declaration of Competing Interest

The authors declare that they have no known competing financial interests or personal relationships that could have appeared to influence the work reported in this paper.

Acknowledgement

The present work was financially supported by National Natural Science Foundation of China (No. 51971148 and 51471110), and the Key Laboratory of Inorganic Coating Materials, Chinese Academy of Sciences (ICM-202003). PKL thanks the support from the National Science Foundation (DMR-1611180 and 1809640) with the program directors, Drs. J. Yang, G. Shiflet, and D. Farkas.

Data availability

The raw/processed data required to reproduce these findings cannot be shared at this time due to technical or time limitations.

References

[1] S. Du, K. Zhang, M. Wen, P. Ren, Q. Meng, Y. Zhang, W. Zheng, Crystallization of SiC and its effects on microstructure, hardness and toughness in TaC/SiC multilayer films, Ceram. Int. 44 (1) (2018) 613–621, https://doi.org/10.1016/j.ceramint.2017.09.220.

[2] Y.F. Zhang, Q. Li, M. Gong, S. Xue, J. Ding, J. Li, J. Cho, T. Niu, R. Su, N.A. Richter, H. Wang, J. Wang, X. Zhang, Deformation behavior and phase transformation of nanotwinned Al/Ti multilayers, Appl. Surf. Sci. 527 (2020) 146776, https://doi.org/10.1016/j.apsusc.2020.146776.

[3] T. Wolfgang, K. David, S. Dominic, F. Qingqing, E.K. Frank, Bias-voltage effect on the TiN nanoparticle injection into magnetron sputtered CrN thin films towards nc-TiN/nc-CrN composites, Appl. Surf. Sci. Adv. 6 (2021), https://doi.org/10.1016/j.apsadv.2021.100149 100149.

[4] H. Dogan, F. Findik, A. Oztarhan, Comparative study of wear mechanism of surface treated AISI 316L stainless steel, Ind. Lubr. Tribol. 55 (2) (2003) 76, https://doi.org/10.1108/00368790310470903.

[5] R. Yigit, E. Celik, F. Findik, S. Koksal, Tool life performance of multilayer hard coatings produced by HTCVD for machining of nodular cast iron, Int. J. Refract. Met. H. 26 (6) (2008) 514–524, https://doi.org/10.1016/j.ijrmhm.2007.12.003.

[6] H. Liang, B.o. Zhang, D. Zhou, X. Guo, Y. Li, Y. Lu, Y. Guo, Effect of Y concentration and film thickness on microstructure and electrical properties of HfO_2 based thin films, Ceram. Int. 47 (9) (2021) 12137–12143, https://doi.org/10.1016/j.ceramint.2021.01.060.

[7] S. Pugal Mani, M. Kalaiarasan, K. Ravichandran, N. Rajendran, Y. Meng, Corrosion resistant and conductive TiN/TiAlN multilayer coating on 316L SS: a promising metallic bipolar plate for proton exchange membrane fuel cell, J. Mater. Sci 56 (17) (2021) 10575–10596, https://doi.org/10.1007/s10853-020-05682-4.

[8] R. Su, D. Neffati, Q. Li, S. Xue, C. Fan, J. Cho, Y. Zhang, J. Li, H. Wang, Y. Kulkarni, X. Zhang, Ultra-high strength and plasticity mediated by partial dislocations and defect networks: Part II: Layer thickness effect, Acta. Mater. 204 (2021) 116494, https://doi.org/10.1016/j.actamat.2020.116494.

[9] W. Yu, W. Li, P. Liu, K.e. Zhang, F. Ma, X. Chen, R. Feng, P.K. Liaw, Silicon-content-dependent microstructures and mechanical behavior of (AlCrTiZrMo)-Si_x-N high-entropy alloy nitride films, Mater. Design. 203 (2021) 109553, https://doi.org/10.1016/j.matdes.2021.109553.
[10] W. Li, P. Liu, Y. Zhao, F. Ma, X. Liu, X. Chen, D. He, Structure, mechanical properties and thermal stability of CrAlN/ZrO_2 nanomultilayers deposited by magnetron sputtering, J. Alloy Compd. 562 (2013) 5–10, https://doi.org/10.1016/j.jallcom.2013.02.020.
[11] A. Saeid, E. Parisa, F. Masayoshi, E. Kaveh, High-entropy ceramics: Review of principles, production and applications, Mater. Sci. Eng. R Rep. 146 (2021) 100644, https://doi.org/10.1016/j.mser.2021.100644.
[12] R. Hahn, M. Bartosik, R. Soler, C. Kirchlechner, G. Dehm, P.H. Mayrhofer, Superlattice effect for enhanced fracture toughness of hard coatings, Scripta Mater. 124 (2016) 67–70, https://doi.org/10.1016/j.scriptamat.2016.06.030.
[13] O.V. Maksakova, S. Zhanyssov, S.V. Plotnikov, P. Konarski, P. Budzynski, A.D. Pogrebnjak, V.M. Beresnev, B.O. Mazilin, N.A. Makhmudov, A.I. Kupchishin, Y. O. Kravchenko, Microstructure and tribomechanical properties of multilayer TiZrN/TiSiN composite coatings with nanoscale architecture by cathodic-arc evaporation, J. Mater. Sci 56 (8) (2021) 5067–5081, https://doi.org/10.1007/s10853-020-05606-2.
[14] R. Yigit, E. Celik, F. Findik, S. Koksal, Effect of cutting speed on the performance of coated and uncoated cutting tools in turning nodular cast iron, J. Mater. Process. Tech 204 (1–3) (2008) 80–88, https://doi.org/10.1016/j.jmatprotec.2007.10.082.
[15] Q. Zhou, S. Zhang, X. Wei, F. Wang, P. Huang, K. Xu, Improving the crack resistance and fracture toughness of Cu/Ru multilayer thin films via tailoring the individual layer thickness, J. Alloy Compd. 742 (2018) 45, https://doi.org/10.1016/j.jallcom.2018.01.282.
[16] P. Ren, K. Zhang, M. Wen, S. Du, J. Chen, W. Zheng, The roles of Ag layers in regulating strengthening-toughening behavior and tribochemistry of the Ag/TaC nano-multilayer films, Appl. Surf. Sci. 445 (2018) 415–423, https://doi.org/10.1016/j.apsusc.2018.03.202.
[17] Z. Guo, D. Ma, X. Zhang, J. Li, J. Feng, Preparation and toughening of a-CuZr/c-ZrN nano-multilayer hard coatings, Appl. Surf. Sci. 483 (2019) 432–441, https://doi.org/10.1016/j.apsusc.2019.03.289.
[18] O. Ozgun, R. Yilmaz, H.O. Gulsoy, F. Findik, The effect of aging treatment on the fracture toughness and impact strength of injection molded Ni-625 superalloy parts, Mater. Charact. 108 (2015) 8–15, https://doi.org/10.1016/j.matchar.2015.08.006.
[19] Z.R. Liu, Y.X. Xu, B. Peng, W. Wei, L.i. Chen, Q. Wang, Structure and property optimization of Ni-containing AlCrSiN coatings by nano-multilayer construction, J. Alloy Compd. 808 (2019) 151630, https://doi.org/10.1016/j.jallcom.2019.07.342.
[20] J. Buchinger, A. Wagner, Z. Chen, Z.L. Zhang, D. Holec, P.H. Mayrhofer, M. Bartosik, Fracture toughness trends of modulus-matched TiN/(Cr, Al)N thin film superlattices, Acta Mater. 202 (2021) 376–386, https://doi.org/10.1016/j.actamat.2020.10.068.
[21] J. Buchinger, N. Koutná, Z. Chen, Z. Zhang, P.H. Mayrhofer, D. Holec, M. Bartosik, Toughness enhancement in TiN/WN superlattice thin films, Acta Mater. 172 (2019) 18–29, https://doi.org/10.1016/j.actamat.2019.04.028.
[22] J.L. Qi, L.P. Wang, Y. Zhang, X. Guo, W.Q. Yu, Q.H. Wang, K. Zhang, P. Ren, M. Wen, Amorphous AlN nanolayer thickness dependent toughness, thermal stability and oxidation resistance in TaN/AlN nanomultilayer films, Surf. Coat. Tech. 405 (2021) 126724, https://doi.org/10.1016/j.surfcoat.2020.126724.
[23] H. Wang, H. Zeng, Q. Li, J. Shen, Superlattice supertoughness of TiN/MN (M = V, Nb, Ta, Mo, and W): First-principles study, Thin Solid Films 607 (2016) 59–66, https://doi.org/10.1016/j.tsf.2016.03.061.
[24] Y. Zeng, Y. Zhen, J. Bian, J. Zhang, J. Pi, G. He, A. Xu, X. Zhang, J. Jiang, Cubic AlN with high thermal stabilities in TiN/AlN multilayers, Surf. Coat. Tech. 364 (2019) 317–322, https://doi.org/10.1016/j.surfcoat.2019.01.031.
[25] Z. Chen, Q. Shao, M. Bartosik, P.H. Mayrhofer, H. Chen, Z. Zhang, Growth-twins in CrN/AlN multilayers induced by hetero-phase interfaces, Acta Mater. 185 (2020) 157–170, https://doi.org/10.1016/j.actamat.2019.11.063.
[26] F. Peng, D. Chen, H. Fu, X. Cheng, The phase transition and the elastic and thermodynamic properties of AlN: First principles, Physica B 403 (23–24) (2008) 4259–4263, https://doi.org/10.1016/j.physb.2008.09.013.
[27] K. Yalamanchili, I.C. Schramm, E. Jiménez-Piqué, L. Rogström, F. Mücklich, M. Odén, N. Ghafoor, Tuning hardness and fracture resistance of ZrN/$Zr_{0.63}Al_{0.37}N$ nanoscale multilayers by stress-induced transformation toughening, Acta Mater. 89 (2015) 22–31, https://doi.org/10.1016/j.actamat.2015.01.066.
[28] W. Chen, M.P. Julio, Y. Yanqing, C. Yip-Wah, Investigation of hardness and fracture toughness properties of Fe/VC multilayer coatings with coherent interfaces, Surf. Coat. Tech. 288 (2016) 179–184, https://doi.org/10.1016/j.surfcoat.2016.01.025.
[29] A.N. Ranade, L.R. Krishna, Z. Li, J. Wang, C.S. Korach, Y.W. Chung, Relationship between hardness and fracture toughness in Ti–TiB_2 nanocomposite coatings, Surf. Coat. Tech. 213 (2012) 26–32, https://doi.org/10.1016/j.surfcoat.2012.10.007.
[30] S. Zhang, D. Sun, Y. Fu, Y.T. Pei, J.T.M. De Hosson, Ni-toughened nc-TiN/a-SiN_x nanocomposite thin films, Surf. Coat. Tech. 200 (5–6) (2005) 1530–1534, https://doi.org/10.1016/j.surfcoat.2005.08.080.
[31] W.C. Oliver, G.M. Pharr, An improved technique for determining hardness and elastic modulus using load and displacement sensing indentation experiments, J. Mater. Res. 7 (6) (1992) 1564–1583, https://doi.org/10.1557/JMR.1992.1564.
[32] G. Qiao, S. Yi, W. Zheng, M. Zhou, Material removal behavior and crack-inhibiting effect in ultrasonic vibration-assisted scratching of silicon nitride ceramics, Ceram. Int. 48 (3) (2022) 4341–4351, https://doi.org/10.1016/j.ceramint.2021.10.229.
[33] T.K. Chen, T.T. Shun, J.W. Yeh, M.S. Wong, Nanostructured nitride films of multi-element high-entropy alloys by reactive DC sputtering, Surf. Coat. Tech. 188–189 (2004) 193–200, https://doi.org/10.1016/j.surfcoat.2004.08.023.
[34] A. Madan, I.W. Kim, S.C. Cheng, P. Yashar, V.P. Dravid, S.A. Barnett, Stabilization of cubic AlN in epitaxial AlN/TiN superlattices, Phys. Rev. Lett. 78 (9) (1997) 1743–1746, https://doi.org/10.1103/PhysRevLett.78.1743.
[35] K. Nikola, L. Lukas, H. David, C. Zhuo, Z. Zaoli, H. Lars, H.M. Paul, G.S. Davide, Atomistic mechanisms underlying plasticity and crack growth in ceramics: a case study of AlN/TiN superlattices, Acta. Mater. 229 (2022) 117809, https://doi.org/10.1016/j.actamat.2022.117809.
[36] Z. Chen, Y. Zheng, Y. Huang, Z. Gao, H. Sheng, M. Bartosik, P.H. Mayrhofer, Z. Zhang, Atomic-scale understanding of the structural evolution in TiN/AlN superlattice during nanoindentation— Part 2: Strengthening, Acta. Mater. 234 (2022) 118009, https://doi.org/10.1016/j.actamat.2022.118009.
[37] Y. Hara, T. Yamanishi, K. Azuma, H. Uchida, M. Yatsuzuka, AlN formation and enhancement of high-temperature oxidation resistance by plasma-based ion implantation, Surf. Coat. Tech. 169 (2003) 359–362, https://doi.org/10.1016/S0257-8972(03)00114-2.
[38] M.S. Wong, G.Y. Hsiao, S.Y. Yang, Preparation and characterization of AlN/ZrN and AlN/TiN nanolaminate coatings, Surf. Coat. Tech. 133 (2000) 160–165, https://doi.org/10.1016/S0257-8972(00)00958-0.
[39] M. Fallmann, Z. Chen, Z.L. Zhang, P.H. Mayrhofer, M. Bartosik, Mechanical properties and epitaxial growth of TiN/AlN superlattices, Surf. Coat. Tech. 375 (2019) 1–7, https://doi.org/10.1016/j.surfcoat.2019.07.003.
[40] M. Wen, H. Huang, K. Zhang, Q. Meng, X. Li, X. Zhang, L. Kong, W. Zheng, Effects of modulation periodicity on microstructure, mechanical and tribological properties of NbN/AlN nanostructured multilayer films, Appl. Surf. Sci. 284 (2013) 331–339, https://doi.org/10.1016/j.apsusc.2013.07.102.
[41] D. Yin, X. Peng, Y.i. Qin, Z. Wang, Template effect in TiN/AlN multilayered coatings from first principles, Ceram. Int. 41 (8) (2015) 10095–10101, https://doi.org/10.1016/j.ceramint.2015.04.104.
[42] I.A. Abrikosov, A. Knutsson, B. Alling, F. Tasnádi, H. Lind, L. Hultman, M. Odén, Phase Stability and Elasticity of TiAlN, Materials. 4 (9) (2011) 1599–1618, https://doi.org/10.3390/ma4091599.
[43] P. Cui, W. Li, P. Liu, K.e. Zhang, F. Ma, X. Chen, R. Feng, P.K. Liaw, Effects of nitrogen content on microstructures and mechanical properties of (AlCrTiZrHf)N high-entropy alloy nitride films, J. Alloy. Compd. 834 (2020) 155063, https://doi.org/10.1016/j.jallcom.2020.155063.
[44] W. Li, K.e. Zhang, P. Liu, W. Zheng, F. Ma, X. Chen, R. Feng, P.K. Liaw, Microstructural characterization and strengthening mechanism of AlN/Y nanocomposite and nanomultilayered films, J. Alloys Compounds 732 (2018) 414–421, https://doi.org/10.1016/j.jallcom.2017.10.244.
[45] J.-K. Park, Y.-J. Baik, The crystalline structure, hardness and thermal stability of AlN/CrN superlattice coating prepared by DC magnetron sputtering, Surf. Coat. Tech. 200 (5–6) (2005) 1519–1523, https://doi.org/10.1016/j.surfcoat.2005.08.099.
[46] Q. Yang, C. He, L.R. Zhao, J.-P. Immarigeon, Preferred orientation and hardness enhancement of TiN/CrN superlattice coatings deposited by reactive magnetron sputtering, Scripta Mater. 46 (4) (2002) 293–297, https://doi.org/10.1016/S1359-6462(01)01241-6.
[47] G. Li, Y. Li, G. Li, Crystallization of amorphous AlN and superhardness effect in VC/AlN nanomultilayers, Thin Solid Films 520 (6) (2012) 2032–2035, https://doi.org/10.1016/j.tsf.2011.09.079.
[48] M. Schlögl, C. Kirchlechner, J. Paulitsch, J. Keckes, P.H. Mayrhofer, Effects of structure and interfaces on fracture toughness of CrN/AlN multilayer coatings, Scripta Mater. 68 (12) (2013) 917–920, https://doi.org/10.1016/j.scriptamat.2013.01.039.
[49] N. Verma, S. Cadambi, V. Jayaram, S.K. Biswas, Micromechanisms of damage nucleation during contact deformation of columnar multilayer nitride coatings, Acta Mater. 60 (6–7) (2012) 3063–3073, https://doi.org/10.1016/j.actamat.2012.02.011.